

A. Szymański<sup>a</sup>, S. Dykas<sup>b</sup>, M. Majkut<sup>b\*</sup>, M. Strozik<sup>b</sup>

## The effects of variable operational parameters on an aero engine labyrinth seals performance

<sup>a</sup> *Cranfield University, Cranfield, Bedfordshire, United Kingdom*

<sup>b</sup> *Institute of Power Engineering and Turbomachinery, Silesian  
University of Technology, Konarskiego 18, 44-100 Gliwice, Poland*

### Abstract

The paper presents the accurate assessment of the amount of gas flowing through three types of aero-engine expander sealing. Structures consisting of straight-through labyrinth seals – with one, two and three fins are considered. The study deploys two independent approaches. The first one focuses on the experimental research using high-precision test section with non-rotating labyrinth seals specimen connected to a high capacity vacuum installation. Experimentally tested seals are of actual size (model to engine scale is 1:1). High accuracy hot-wire anemometry probes, and orifice plate are deployed to evaluate the flow indicators accurately, allowing for comparison of different sealing structures. The second approach uses quasi-two-dimensional axis-symmetric, steady-state Reynolds averaged Navier Stokes (RANS) computations to simulate the flow field. Various meshes and turbulence models were tested, presenting capabilities as well as limitations of specific computational approaches. The experimental and computational results were compared with literature data, showing a good agreement regarding overall trends, yet underlining some local discrepancies. This paper brings two significant findings. The 2D RANS methods tend to overestimate the leakage when compared with experimental results, and the difference is more significant for advanced arrangements. There is a notable difference between the performance of labyrinth seal with one fin and structure with two and three fins. In some operational areas, one-finned seal performs better than more advanced ones, reducing the leakage more effectively. This feature of one finned seal is not intuitive, as one would expect it to perform worse than a seal with two or three fins.

---

\*Corresponding Author. E-mail adress: miroslaw.majkut@polsl.pl

**Keywords:** Labyrinth seals; Experiment; Turbomachinery; Gas turbine; Validation

## Nomenclature

$A$	–	surface area
$b$	–	fin width
$C_D$	–	discharge coefficient
$c_{AX}$	–	axial velocity above the fin tip
$D$	–	diameter
$h$	–	fin tip width
$L$	–	length
$\dot{m}$	–	mass flow rate
$P$	–	pressure
$R$	–	individual gas constant
$s$	–	clearance size
$T$	–	temperature
$t$	–	fin pitch
$u$	–	circumferential velocity of rotor tip
$y^+$	–	nondimensionalized wall normal distance

## Greek symbols

$\psi$	–	flow function
$\pi$	–	pressure ratio
$\gamma$	–	adiabatic exponent

## Subscripts

$id$	–	ideal
$s$	–	static
$0$	–	total

## Abbreviations

HWA	–	hot wire anemometry
-----	---	---------------------

# 1 Introduction

An efficiency of aero engines expanders highly depends on the secondary flows distribution. The major factor contributing to stage efficiency loss is the rotor tip leakage. It is of utmost importance to control it and keep it as low as necessary. Among a large variety of seals applied in turbomachinery to guarantee required confinement of the main flow path, labyrinth seals perform well concern-

ing resistance to wear, high temperature and pressure, and destruction resulted from fouling [1]. However, the flow reduction is as much as four-fold lower when compared to state-of-the-art solutions like brush seals, wafer seals, finger seals, etc. [2]. Relatively high leakage is the reason for the necessity of research and optimisation of the labyrinth sealing structures regarding flow reduction as well as adequate distribution of secondary air in the machine. Another important issue is sealing behaviour during the engine operation. The clearance varies during different stages of the mission – it drops after take-off, then rises slightly during cruise, and ramps up during deceleration. The designed estimated clearance variation between low pressure (LP) turbine tip and casing are in the range of 0.5 to 2 labyrinth fin tip width [1]. A rise of the leakage in the turbine from 3% to 4.5% of main flow rate, results in the rise of the downstream temperature up to 303 K on average. This phenomenon, on the other hand, limits the machine lifetime due to the creep occurrence. Experimental studies of labyrinth seals flow are in the interest of researchers since 1970 [3]. They focused both on the rotational configurations, taking the circumferential velocity of a rotor into account and simplified approach, without circumference of the specimen and its movement. They showed a strong effect of the clearance size, the number of fins and the fins shape on the leakage. Further studies done individually by Waschka [4] and Paolillo [5] present that the effect of rotational velocities is irrelevant when the circumferential velocity of rotor tip,  $u$ , is lower than an axial velocity above the fin tip,  $c_{AX}$ , and condition  $u/c_{AX} < 1$  is met. This assumption is true for most of the aero engine low pressure expanders, often characterising with rotational speed of 2000–3000 rpm, as well as for all heavy duty gas and steam turbines (1500–1800 or 3000–3600 rpm). For this range of revolutions, the effect of rotational velocity is limited, and does not have to be taken into account. Research presented by Braun [6] shows experimental results for the labyrinth with three straight fins, done on the stationary test section, supplied with high-pressure air. The investigated geometry was scaled up three-fold and five-fold, and compared to the reference geometry. The results between original geometry and rescaled one varied between 5–10%. This difference is significant, for instance when optimisation is targeted [7], and flow rate reductions of similar order of magnitude are taken into account. For this reason, in this study the investigated geometry is kept in the same scale as real-operating one. As the labyrinth seals are relatively small structures, this requirement can be very challenging to meet, due to significant requirements towards the manufacturing tolerance and measurements accuracy. Experimental and computational work on the labyrinth seals with different number of fins and their geometry underline that the flow characteristics

strongly depend on their dimensions, and what is more relevant – the relation between them. Because of scaling limitations, fins dimensions adequate for LP turbine stages are taken into account [8]. Moreover, the fact that most of the experimental research [9,5,10] focus on a one, specific geometry of labyrinth seal, with little variations additionally motivates this paper. It is difficult to find out what would be the impact of geometry change within the operational envelope – like clearance size on the leakage. The literature results concerning labyrinth seals flow are often inconsistent, and present various trends. Especially results with 3–5 fins present contrasting tendencies – the discharge coefficient can be either rising or dropping with the function of clearance size and pressure load [6].

The purpose of this paper is to present multivariant analysis, generating a considerable dataset which is a source of data for further studies aiming for the comparison with computational fluid dynamics (CFD) and analytical methods. Analytical models were the first to determine the flow through the labyrinth seals and still are used by engineers in modified version [11,12]. The experiment is followed by CFD study, presenting the methodology for efficient and reliable leakage assessment. The paper is organised as follows: in the first section, we describe test section and test rig used to provide data to validate the modelling approaches. The CFD code, meshing and turbulence model selection are then described, and the CFD results are compared with measurements and historical data. A further quantitative study of the flow in the different labyrinth structures is developed based on the experiment and validated computational method. Finally, we show comparisons of the three labyrinth seal structures concerning the leakage characteristics and discuss the trends.

## 2 Problem formulation

Although the labyrinth seals have been a subject of research for the past 40 years, there are still few comprehensive reports on the effect of fundamental parameters change in simple labyrinth seal, especially with a low number of fins (1–3). Most of the authors focus on one specific structure without more global overview. On the other hand, turbomachinery designers, still use analytical methods of evaluation of leakage in turbomachinery, based on research conducted more than 40 years ago [11,13]. This fact creates a gap between the data available in public domain, and the majority of research undertaken in the past, without any update. Work done by Kearon and continued by Zimmerman may serve as an example here. Kearon in 50 conducted experimental research [13], and its results were used 30 years later by Zimmerman [11,12] to create an analytical model for

evaluation of the stepped labyrinth seals flow characteristics. For this reason, the one fin case was deployed as a validation case in this study. Additional tests were carried out for labyrinth seals with two and three fins, working in the same conditions. Modern experimental and computational methods allowed for verification and a better understanding of older results – quite often burdened with some uncertainty. The most convenient and reliable method for comparison of different sealing structures, including those tested in laboratory and seals applied in real operating engines, is by comparing non-dimensional flow indicators. In the case of labyrinth seals, the most popular ones are discharge coefficient,  $C_D$ , and flow function,  $\psi$ . Discharge coefficient is the ratio between the actual flow rate, measured or calculated, divided by mass flow rate which would occur in isentropic flow conditions

$$C_D = \frac{\dot{m}}{\dot{m}_{id}}, \quad (1)$$

where ideal mass flow defines as:

$$\dot{m}_{id} = \frac{p_0 A}{\sqrt{T_0}} \sqrt{\frac{2\gamma}{R(\gamma-1)} \left[ \left(\frac{1}{\pi}\right)^{2/\gamma} - \left(\frac{1}{\pi}\right)^{(\gamma+1)/\gamma} \right]}. \quad (2)$$

Here an overdot denotes differentiation with respect to time. The discharge coefficient describes the effectiveness of the leakage mass flow reduction as a function of pressure ratio. This approach has been successfully presented in [4,6,14,15].

The presented pressure ratio is a measure of sealing load, and is described as a ratio of total pressure at the inlet to the sealing structure related to static pressure downstream of the last fin

$$\pi = \frac{p_0}{p_s}. \quad (3)$$

In further sections, the procedure for determination of  $p_s$  is introduced. Another widely used parameter [3,16] describing labyrinth seals characteristics is flow function. It denotes the mass flow related to the flow area and total inlet parameters. Unlike the discharge coefficient, it is independent of pressure ratio and is sometimes referred to as non-dimensionalised or reduced mass flow rate

$$\Psi = \frac{\dot{m}\sqrt{T_0}}{Ap_0}. \quad (4)$$

Additionally, to compare the sealing effectiveness on the energy dissipation, flow function under perfect conditions is introduced. It presents the maximal dimen-

sionless flow, which can be obtained in given conditions

$$\Psi_{ideal} = \sqrt{\frac{2\gamma}{R(\gamma-1)} \left[ \left(\frac{1}{\pi}\right)^{2/\gamma} - \left(\frac{1}{\pi}\right)^{(\gamma+1)/\gamma} \right]}. \quad (5)$$

### 3 Experimental apparatus

The experimental part of the research was carried out using vacuum installation located in the Turbomachinery Laboratory of the Institute of Power Engineering and Turbomachinery of the Silesian University of Technology (SUT). The vacuum is generated by roots air blower, with a capacity of 600 Nm<sup>3</sup>/min (0.2 kg/s), connected directly to the 3 m<sup>3</sup> pressure vessel. The lowest available pressure at the inlet to the air blower (outlet of the test section) is 50 kPa (absolute). It allows reaching maximal pressure ratio up to 2. The total volume of the installation (vessel and pipelines) exceeds 3.5 m<sup>3</sup>. This value is relatively high compared to expected flow rates, which allows keeping the parameters downstream of the test section stable. Figure 1 shows the scheme of described installation.

Secondary air is delivered from the surroundings, via two automatically regulated valves. One of them is of internal diameter 100 mm (diameter nominal, DN 100), and the remaining one of DN 50. Air flowing through valves has an impact on the pressure inside the vessel, which on the other hand forces the air flow in the test section. The mentioned regulation method guarantees reliable and repeatable adjustment of pressure downstream of the rig. On the inlet side of the test rig, the air is sucked via 4 m long pipeline ( $L/D$  ratio 40), which indicates satisfactory conditions for flow measurement realised by hot wire anemometry (HWA) probe no. 1. (point 1b in Fig. 1). The mass flow is also measured downstream in the test section – via HWA probe no. 2 and ISA orifice plate, allowing for very accurate mass flow determination. In both cases the HWA probe was Schmidt flow sensor SS 20.500 Ex. Located in the longitudinal axis of pipeline it allowed for the indirect mass flow determination, based on the local velocity (the average velocity was obtained with profile coefficient provided by the manufacturer) and inlet air parameters. The distances between mass flow sensors were designed to be at least  $L/D = 10$ , to make sure the velocity profile is adequate, and does not distort the outcomes.

#### 3.1 Measurement procedure and results evaluation

Flows through labyrinth seals are highly turbulent. They characterise with sudden flow acceleration, strong vortices and large pressure and velocity gradients.

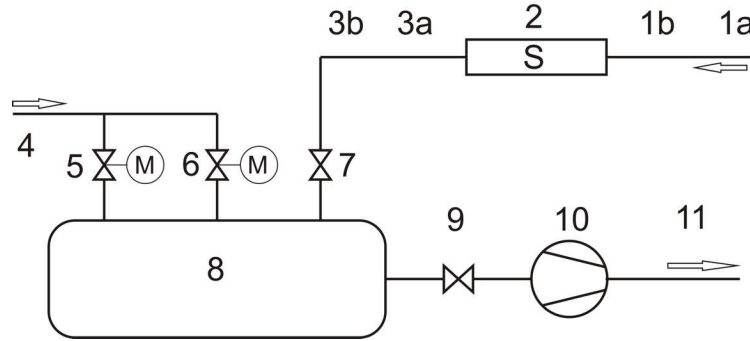


Figure 1: Scheme of vacuum installation for labyrinth seals testing in the SUT: 1a – inlet to the test rig ( $T_0$ ,  $p_0$  – evaluation), 1b – HWA probe no. 1 (ambient conditions), 2 – test section, 3a – HWA probe no. 2 (7 m downstream the test rig, low pressure conditions), 3b – ISA orifice plate, 4 – secondary air inlet, 5 – DN 100 valve, 6 – DN 50 valve, 7, 8 – 3 m<sup>3</sup> pressure vessel, 9 – cut-off valves, 10 – roots air blower, 11 – exhaust to the environment.

The flow accelerates in the labyrinth seal clearance, where it can reach high Mach number and then it expands in a cavity between fins, which is the mechanism of pressure losses. In presented experimental studies, the deployed test section characterises with very high aerodynamic inertia, guaranteeing stable pressure values on the test rig outlet. On the other hand, the longer time to achieve the steady-state parameters is necessary. It was established, that steady state is obtained when the time-averaged mass flow in three described measurement points (see 1b, 3a, and 3b in Fig. 1) is the same for at least one minute. Finally, the time to derive one operating point was 90 s, which was equivalent to 4500 samples. The time to obtain one characteristics curve was around 100 min, including the measurement time, as well as time to reach stable pressure in the outlet zone after the valve position changes. Measurement series were repeated many times – at least 6-7, to assure the result is accurate and repeatable. Presented measurement approach is sufficient for the given problem, even if a measurement campaign was carried on in a different time, followed by test section reassembly and clearance adjustment. The clearance measurement was performed using blade feelers, with the accuracy of  $\pm 0.005$  mm. Pressure measurement was realised with the accuracy of  $\pm 256$  Pa, and temperature measurement with  $\pm 0.1$  K. The mass flow rate evaluated with HWA probes characterised with uncertainty below 1%, and with the orifice plate below 2%. Combining all measurement errors, uncertainties were then determined (Tab. 1). Parameters analysed were: pressure ratio,  $\pi$ , discharge coefficient,  $C_D$ , and flow function,  $\Psi$ . As values of  $\Delta C_D$  and  $\Delta \Psi$  were almost the

same, the table presents combined results for both flow indicators. The pressure ratio uncertainty is negligible ( $\Delta\pi < 0.1\%$ ).

Table 1: Mean measurement uncertainties of flow indicators.

Clearance size $s$ , mm	Mean uncertainty $\Delta C_D$ and $\Delta\Psi$ , %
1.50	$\pm 0.6$
1.00	$\pm 1.0$
0.75	$\pm 1.9$
0.40	$\pm 2.7$

### 3.2 Subject of research

A wide range of experimental research on the turbomachinery-intended labyrinth seals was performed in the SUT in the past few years [8,17–19]. They included experimental, CFD studies and optimisation. This paper presents the approach of the test section with circular labyrinth seals specimen (Figs. 2 and 3), briefly given in [17], supported by comprehensive CFD campaign. Vacuum installation described in the previous paragraph is connected to the test section. It characterises with non-complex design – the labyrinth seals probes were installed in the circular housing. The labyrinth specimen is not rotating and the effects of walls movement are neglected. This approach is proved to be valid if the air axial velocity above the fin is lower than the circumferential velocity of the fin tip, and the condition  $u/c_{AX} < 1$  is met [4,5]. This happens to be truth in many turbines locations, especially in modern jet engines and aero-derivative gas turbines, where the pressure ratios are significant (compressor discharge pressure seal, expander stages seals), and the rotational velocity is low. On the other hand, the proposed approach with a non-rotating specimen allows for a relatively straightforward experimental test of the effects of the geometrical parameters, such as a number of fins or clearance size. Due to its circular outline, it required very accurate manufacturing, especially concerning the axial symmetry. Clearance adjustment determination was realised by replacement sleeves inside the test rig housing. Described compartments, were made in High-Precision Manufacturing Laboratory of SUT, with the tolerances within  $\pm 0.005$  mm. The clearance size was controlled using high precision blade feelers, with accuracy  $\pm 0.005$  mm. Proposed test rig conception simplified the measurement process, as well as shortened its assembly time. To predict the pressure ratio (load) of the labyrinth seal, static pressure



in three points located with  $120^\circ$  distance 30 mm downstream of the last fin was measured. Then those three values were averaged and used for pressure ratio determination. It was revised in each and every point if the measurement values deviated from the average. Any differences between readings in any angular location were less than pressure sensor accuracy ( $\pm 256$  Pa), meaning the static pressure was uniform in the outlet region. Based on the average static pressure in given location, the pressure ratio was then evaluated. The lack of side walls, frequently seen in linear test rigs [15,20,21] eliminates the impact of boundary layer generation on the side walls and possible leakages. The CFD study showed constant static pressure in the area downstream of the fins.

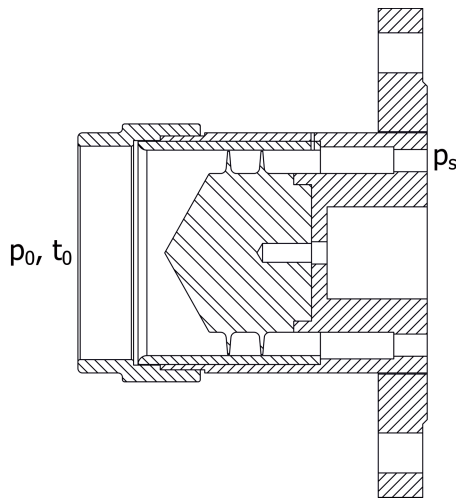


Figure 2: Test rig cross-section.

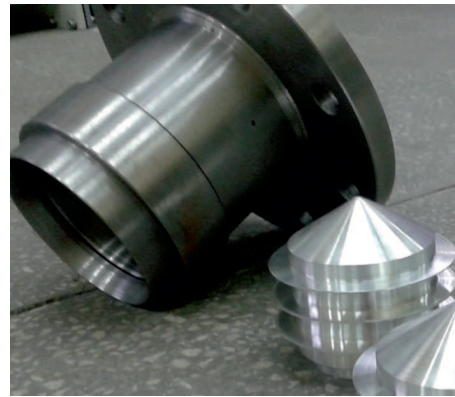


Figure 3: Circular labyrinth seal specimen.

The subject of research were three labyrinth seals configurations. Figure 4 and Tab. 2 presents details of investigated cases. For clarity, we show relative dimensions, helping to place given results among those seen in literature data, where specific parameters are neglected. Moreover, in the case of single-finned labyrinth seal, the results were compared with literature data, coming from [13,16]. Adopted fin height and spacing dimensions are typical for low-pressure gas turbine/aero-engine expander stages solutions ( $\phi 1200$ – $1400$  mm). The relative clearance size in this study is between  $s/b = 0.625$ – $1.875$ , while the most common range for turbomachinery applications is  $0.5$ – $2$ . [2]. The case with one fin was treated with particular attention – the results were compared with the literature results delivered by Kearon [3] and Stocker [13].

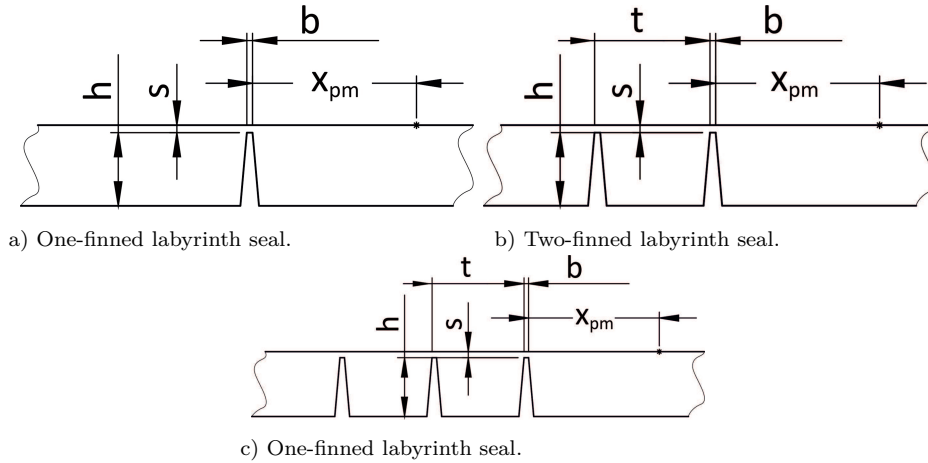


Figure 4: Cross sections of investigated labyrinths.

Table 2: Dimensions of investigated specimens.

$h$	10 mm	$h/b$	12.5
$s$	0.5–1.5 mm	$s/b$	0.625–1.875
$t$	15 mm	$t/b$	18.75
$b$	0.8 mm	–	
$x_{pm}$	30 mm	–	

The parameter  $x_{pm}$  describes the distance between the last fin and the point of static pressure measurement. For every configuration, it was constant. In the case of CFD calculations, the pressure ratio was determined in the same manner – the stagnation pressure at the inlet was related to the pressure in the point 30 mm downstream of the last fin.

### 3.3 One fin labyrinth seal results

Along with the experimental research, a CFD study was conducted. The quasi 2D analysis of flow field characteristics is carried out employing commercial CFD software Ansys CFX 17, with the Reynolds-averaged Navier-Stokes (RANS) approach. Based on literature review, it is difficult to assess which turbulence model is sufficient to determine the flow parameters correctly. Many researchers [9,21,22] use  $k-\varepsilon$ , or  $k-\varepsilon$  re-normalisation group (RNG) methods, and on the other hand,

some works [14,21,23] propose using  $k\text{-}\omega$  shear stress transport (SST) model. Those two approaches differ significantly concerning their application. There are also recommendations towards large eddy simulation (LES) application for robust flow field resolution, including unsteady phenomena [24,25]. For those reasons, a detailed mesh and turbulence study has been introduced. The case selected for mesh study is the seal with one fin, and the clearance size  $s = 1$  mm. Boundary conditions corresponded with experimental parameters: the total temperature and pressure at inlet were set at 293 K and 100 kPa (absolute) respectively, with inlet turbulence intensity equal to 5%. The static outlet pressure varied in the range 50–95 kPa, with the 5% blending factor, to achieve desired pressure ratio. The working fluid was dry air, treated as an ideal gas, with Sutherland formulae for viscosity evaluation. Walls were modelled as adiabatic and hydraulically smooth. Nine different mesh sizes were taken into account, with  $44 \times 103$ ,  $88 \times 103$ ,  $183 \times 103$ ,  $282 \times 103$ ,  $440 \times 103$ ,  $636 \times 103$ ,  $972 \times 103$ ,  $2005 \times 103$ , and  $3500 \times 103$  nodes. Each one was tested with following turbulence models:  $k\text{-}\omega$  (SST),  $k\text{-}\varepsilon$ ,  $k\text{-}\varepsilon$  explicit algebraic Reynolds stress models (EARSM) and RNG  $k\text{-}\varepsilon$ . The mesh resolution was changed locally, especially in the area above the fins and within the boundary layer, not globally. A criterion for termination of the calculation was the stability of the mass flow rate, set as 0.01%. Figure 5 presents the calculation domain with boundary conditions. As planar 2D geometries cannot be resolved in solver directly, the quasi 2D approach was deployed. CFX solver treats very thin 3D geometry, with one element in cross direction, as 2D one [26]. Figure 6 presents adopted mesh details, with  $972 \times 103$  nodes, and parameter  $y^+ < 1$  (nondimensionalized wall normal distance).

More details on the geometry simplification and aspects of turbulence modelling were presented in [17]. The mesh study showed that with the rise of mesh elements, the mass flow rate decreases, and stabilises around  $C_D = 0.66$  (Fig. 7). The only exception here is the  $k\text{-}\varepsilon$  model, which the highly overestimated leakage rate. It is worth mentioning that  $k\text{-}\varepsilon$  and  $k\text{-}\varepsilon$  EARSM did not fulfil the required convergence concerning flow stability, characterising with the fluctuations in the range of  $\pm 0.03C_D$ . In all the cases simulations overestimated the leakage. However, the discrepancy value was around 2–3%, apart from the  $k\text{-}\varepsilon$  and  $k\text{-}\varepsilon$  EARSM models where the discrepancies reached 15% and 6%, respectively. Based on this experience, and the approach observed in the literature, we adopted  $k\text{-}\omega$  SST for further calculations. As a result of the mesh study, the resolution method resulting in  $972 \times 103$  was selected for further calculations.

Because of significant differences between results obtained using the  $k\text{-}\omega$  SST turbulence model and  $k\text{-}\varepsilon$ , further study was conducted. The main reason behind

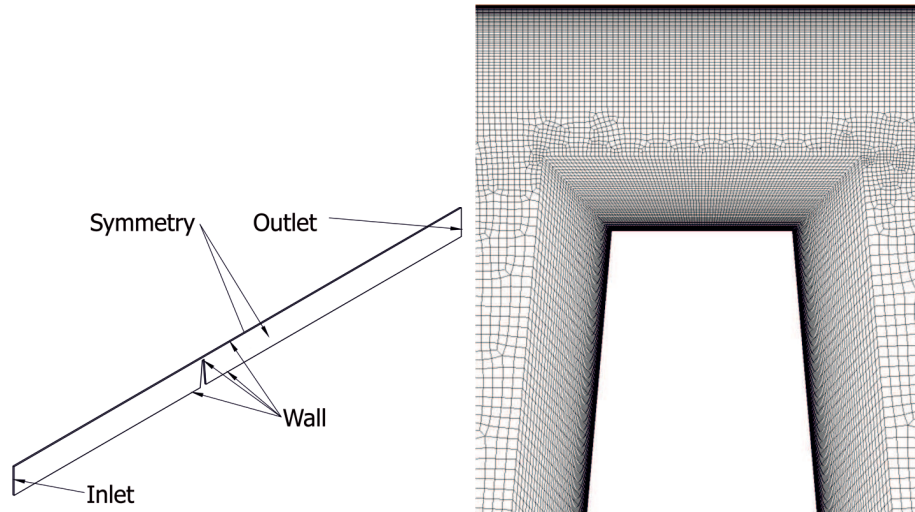


Figure 5: Quasi-2D calculation domain with boundary conditions.

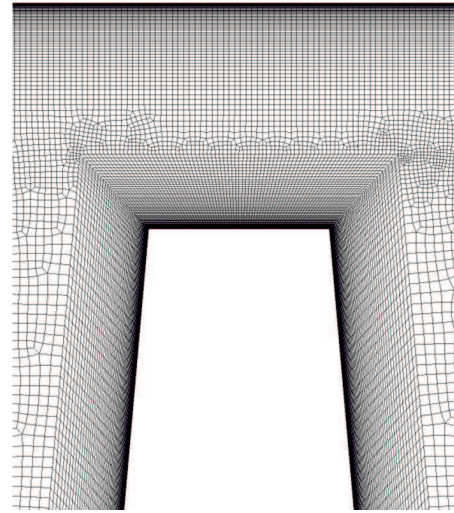


Figure 6: Adopted mesh details –  $972 \times 103$  nodes.

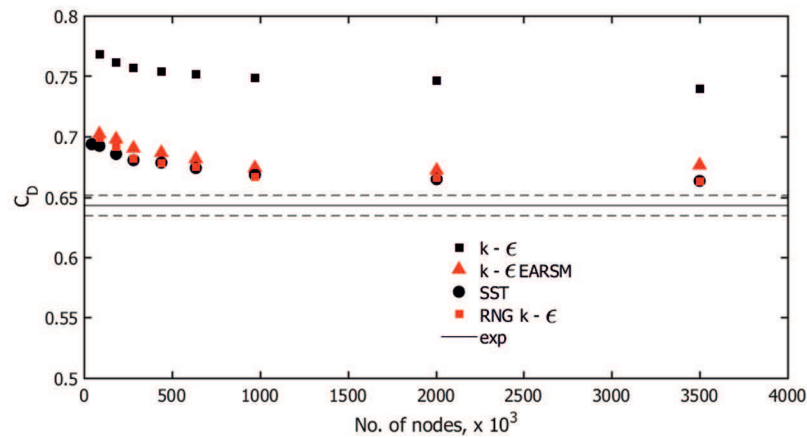


Figure 7: Mesh and turbulence study.

it is the fact that many of authors emphasise that  $k-\epsilon$  model can be utilised in flows in narrow channels [10,20,21], like labyrinth seals.

In Figs. 8 and 9 velocity distribution and streamlines for two cases are compared – using SST and  $k-\epsilon$  turbulence model, in the one fin labyrinth seal with

the clearance  $s = 1$  mm. The  $k-\varepsilon$  turbulence model did not reproduce the vortex structure above and downstream of the fin. The flow separation above the fin caused by the sharp edge is the main mechanism of pressure losses, and therefore leakage limitation. This type of behaviour was previously observed in experimental research [27] and is reproduced well by  $k-\omega$  SST turbulence model. The SST predicts lower expansion angle than the  $k-\varepsilon$  model (Fig. 8), which is caused by different near-wall separation modelling [28].

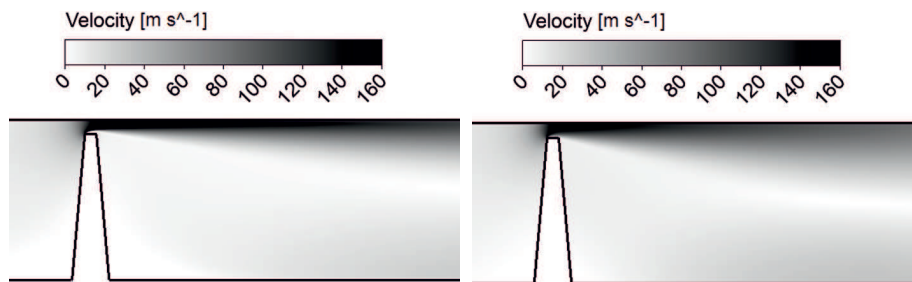


Figure 8: Axial velocity distribution SST – left,  $k-\varepsilon$  right-hand picture.

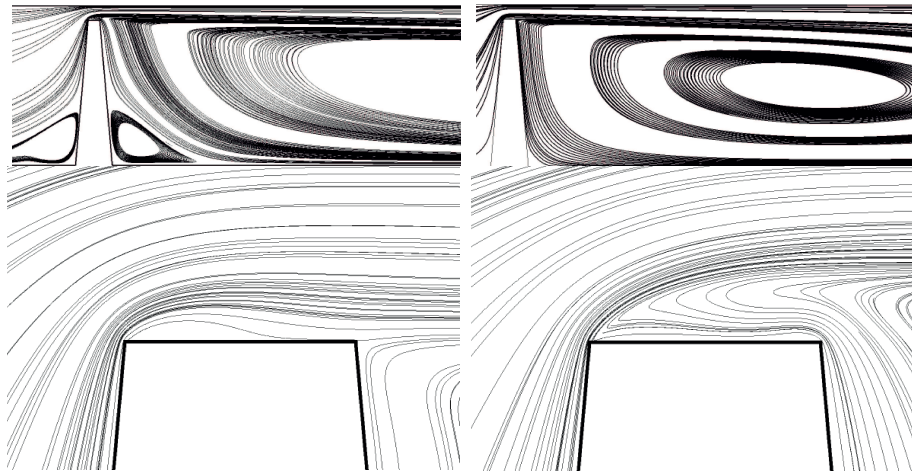


Figure 9: Streamlines SST – left,  $k-\varepsilon$  right-hand picture.

The presented calculations methodology is sufficient for determination of flow indicators in the presented labyrinth seal. Taking under consideration an error being a result of simplification of the geometry, (about 2–3% of  $C_D$ ), differences between the results of calculations and the experiment (1.5–3.5%) and the

measurement uncertainties, the robustness of the presented method is acceptable. Therefore, the proposed calculation scheme basing on the quasi-2D RANS calculation with  $k-\omega$  SST turbulence model is adopted for further calculations, presented in following chapters.

### 3.4 One fin labyrinth seal results

One fin labyrinth seal testing has never been notably presented in the literature. Some research has been done by Kearton (1952) [13] and Tipton (1986) [16]. However, the limited number of information given in cited papers, and the fact they were conducted more than 30 years ago, underlines the necessity of cross-checks. Although labyrinth seals with one fin are not common in turbomachinery, their characteristics are important for the assessment of more sophisticated structures. The analytical model developed by Zimmermann [11,12] may serve as an example here. It assumes the same total pressure drop on every fin of the stepped labyrinth seal, based on the measurement results delivered by Kearton, to estimate the leakage in the stepped labyrinth seals.

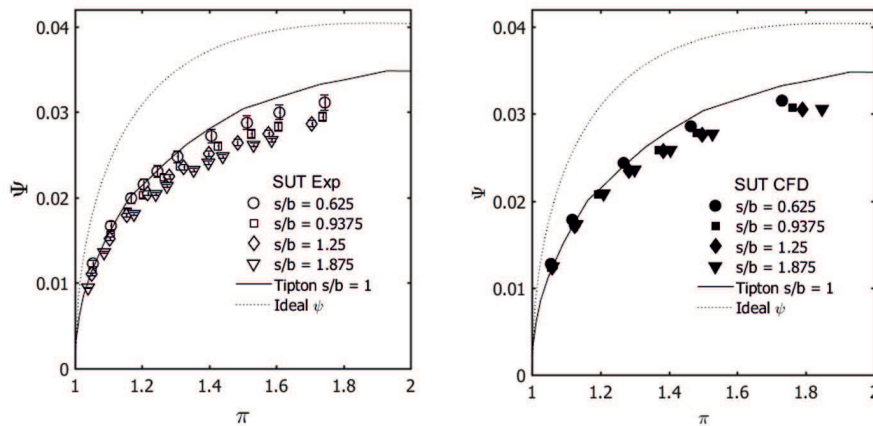


Figure 10: Flow function,  $\Psi$ , as a function of pressure ratio,  $\pi$ . One finned labyrinth seal case. Comparison with Tipton [16] results.

Using correction factor, dependent on the fins geometry, it allows for determining the flow indicators in a wide range of pressure ratio, keeping the process short and effective. The accuracy of this method is estimated to be below 5% [11,12]. In the research done by Kearton, flow behaviour of one fin labyrinth seals was tested as a function of pressure ratio and relative clearance size,  $s/b$ . Unfortunately,

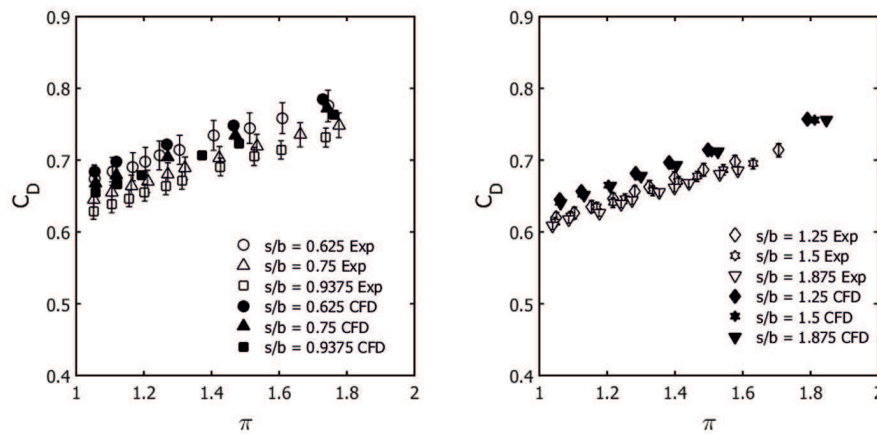


Figure 11: Discharge coefficient,  $C_D$ , as a function of pressure ratio,  $\pi$ . One finned labyrinth seal case. Experimental and CFD results.

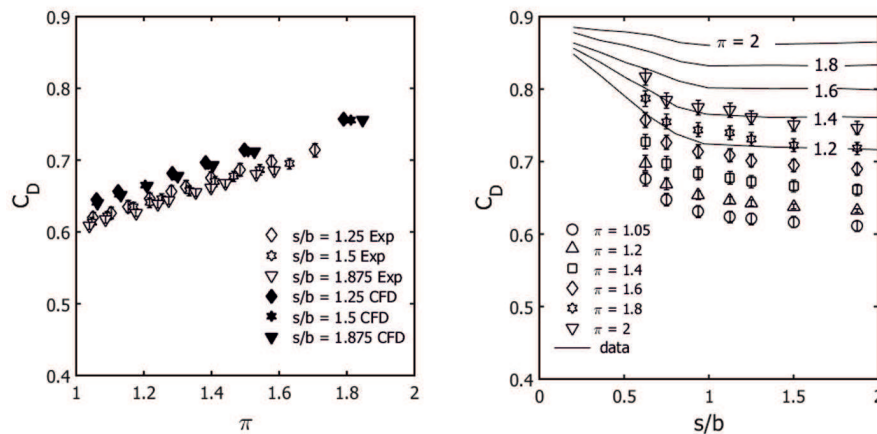


Figure 12: Discharge coefficient,  $C_D$ , as a function of relative clearance,  $s/b$ . One finned labyrinth seal case. Experiment and CFD results compared with Kearton [13] results.

there are no details on the geometry or working fluid parameters mentioned in his paper. Paper by Tipton [16] describes results of an experimental inquiry of various configurations of labyrinth seals, including one fin geometry. The inlet fluid parameters ( $T_0 = 295$  K,  $p_0 = 100$ – $200$  kPa (absolute)) are similar to parameters in the SUT test section ( $T_0 = 293$ – $303$  K,  $p_0 = 100$  kPa (absolute)). Table 3 presents dimensions of compared geometries. Some similarities are found – SUT

geometry is scaled up by the factor of two, compared to Tipton geometry. Based on Braun experiences with scaling labyrinth seals geometries [6], the expected results should not vary more than 10% due to scaling.

Table 3: Tested one fin labyrinth seal geometries details.

Parameter	Symbol	SUT	Tipton	SUT/Tipton
Clearance	$s$	0.5–1.5 mm	0.254 mm	2–6
Fin height	$h$	10 mm	5.08 mm	2
Fin tip width	$b$	0.8 mm	0.254 mm	3.15
Relative clearance	$s/b$	0.625–1.875	1	–

Figures 10, 11, and 12 show results of the experiment and CFD calculation of one fin labyrinth seal. Results are presented as flow function,  $\Psi$ , and discharge coefficient,  $C_D$ , as the function of pressure ratio,  $\pi$ . Reference geometry presented results tendencies similar to those of Stocker. However, the literature results were up to 10% higher than presented ones (Fig. 10). In the range of low-pressure ratios (1–1.3), the discrepancies between Stocker and own data are negligible. For pressure ratio higher than 1.3 they rise up to 10%. However, one should keep in mind that since presented results were obtained for the geometry scaled up twice compared to the Stocker geometry, so some minor differences in the range of 5–10% may occur. At low values of relative clearance ( $s/b < 1$ ), differences between consecutive measurement series are visible, while for higher gaps ( $s/b > 1$ ) the differences between them decline, and fall in the range of  $0.02C_D$ . This behaviour is relevant both for experimental and CFD results. Calculations results present a fair agreement with the experiment data – average discrepancy is in the range of 1.5–3.5% of measured value, with better agreement for low clearances.

Obtained results were also compared with data published by Snow [13]. Flow trends obtained from experiment and CFD calculations present the same tendencies as previously published in the literature (Fig. 12). Unlikely as in configuration with two or more fins, the discharge coefficient  $C_D$  drops as the clearance rises. The literature data are higher by 7–10% compared to own results, but considering the fact the information about the geometry and air parameters are limited, results are satisfying. Presented discrepancies underline the necessity of an update and improvement of cited results – especially if the presented results are further applied for more sophisticated models.



### 3.5 Two and three fins labyrinth seal results

This paragraph presents the experimental and CFD results for two and three-finned seals. They predict an increase of the discharge coefficient with the pressure ratio and clearance size. This behaviour is different when compared with one fin seal, where the trends are in the opposite. The described tendency, of the growth of leakage together with pressure ratio, is reasonable. However, there are some studies presented in the literature showing opposite tendencies for analogous structures, with labyrinth seal with three fins and clearance in the range 0.3–1 mm, indicating the reduction of leakage as the load rises [6]. The case with two fins shows that  $C_D$  values are in the range of 0.57 to 0.75, for the relative clearance sizes ( $s/b = 0.625$ – $1.875$ ) and pressure ratio 1–2 (Fig. 13). An excellent agreement of CFD results is found for the low clearance cases (1–2%), with higher over-estimation at higher gaps, reaching up to 4–5%. Figure 14 shows flow characteristics of the three-finned geometry, presenting lower leakages when compared with the previous cases. The  $C_D$  varies from 0.47 to 0.70, depending on the clearance size and the load. Again, relatively low discrepancies were noticed for cases with small clearances. However, they rise to 9% for the case with the highest gap. In general the proposed CFD calculation model tends to overestimate the results. On the other hand, the CFD results predict the global trends and so called delta-effect of more complex geometry application well.

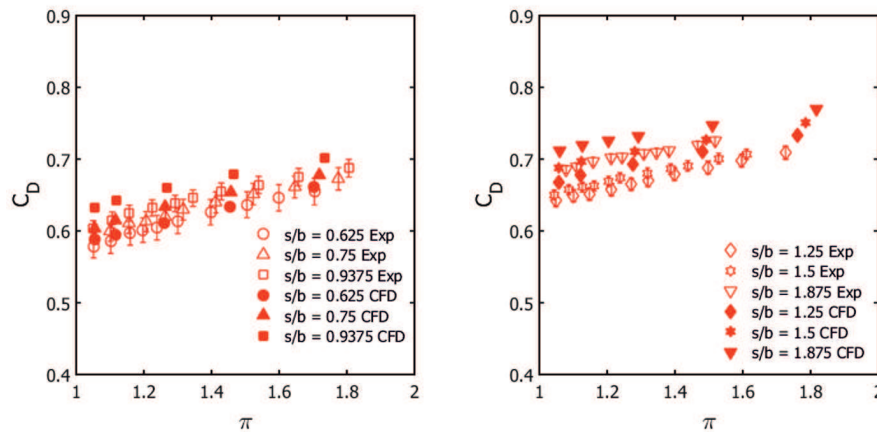


Figure 13: Discharge coefficient,  $C_D$ , as a function of pressure ratio,  $\pi$ . Experiment and CFD results compared with literature data for two-finned labyrinth seal case.

The results suggest the presence of particular regimes where the leakage relies more on the operating parameters, like load or gap size rather than on the sealing

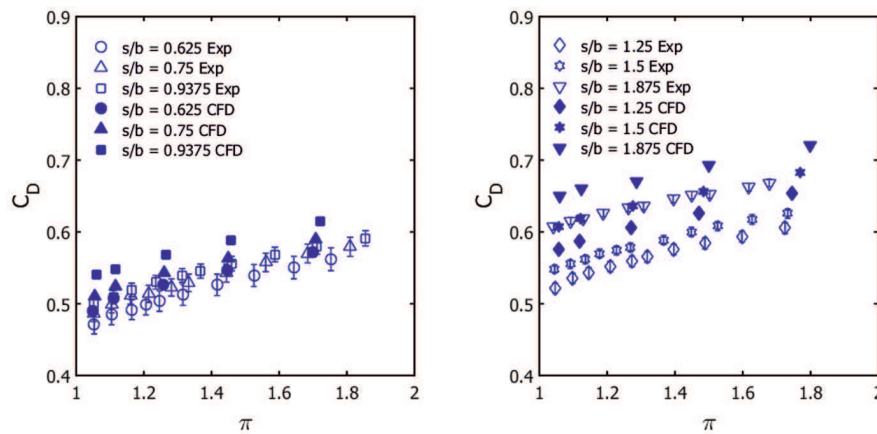


Figure 14: Discharge coefficient,  $C_D$ , as a function of pressure ratio,  $\pi$ . Experiment and CFD results compared for three-finned labyrinth seal case.

structure and number of fins (Fig. 15). For this reason, all examined sealing structures were compared concerning the effect of the relative clearance on the leakage, for four pressure ratios. On each chart, all three tested structures are compared. The following tendency can be observed – as discharge coefficient line for one-finned case intersects with results line of configurations with a higher number of fins, above certain clearance size, it may provide lower leakage than more complex structures. In the presented case, when relative clearance,  $s/b$ , is higher than 1.2 at low-pressure ratios ( $\pi = 1.1$ ), up to 1.5 for the high-pressure ratio ( $\pi = 1.7$ ), one-finned labyrinth seals shows lower leakage (Fig. 15a,b) than the sealing with two fins. The similar tendency is observed in the case with three fins. However, the intersection point shifts towards higher relative gap value, and finally at high-pressure ratios, the intersection is estimated to occur at  $s/b = 2$  – which is the highest considered gap size in turbomachinery (Fig. 15c, and 15d). Nonetheless, in range of low clearance values  $s/b = 0.5$ –1, configurations with two and three fins present leakage lower by up to 20–40% respectively, compared with the geometry with one fin only. Results obtained using CFD are somewhat overestimated – especially in the case with three fins the discrepancy reaches up to 9%. The CFD results indicate the same tendencies of discharge coefficient as experiment, yet the characteristics intersection point may be shifted toward lower relative clearance values.

The differences in flow physics dictate the opposite flow characteristics of the structure with two and one fins, when compared with the one-finned structure. In

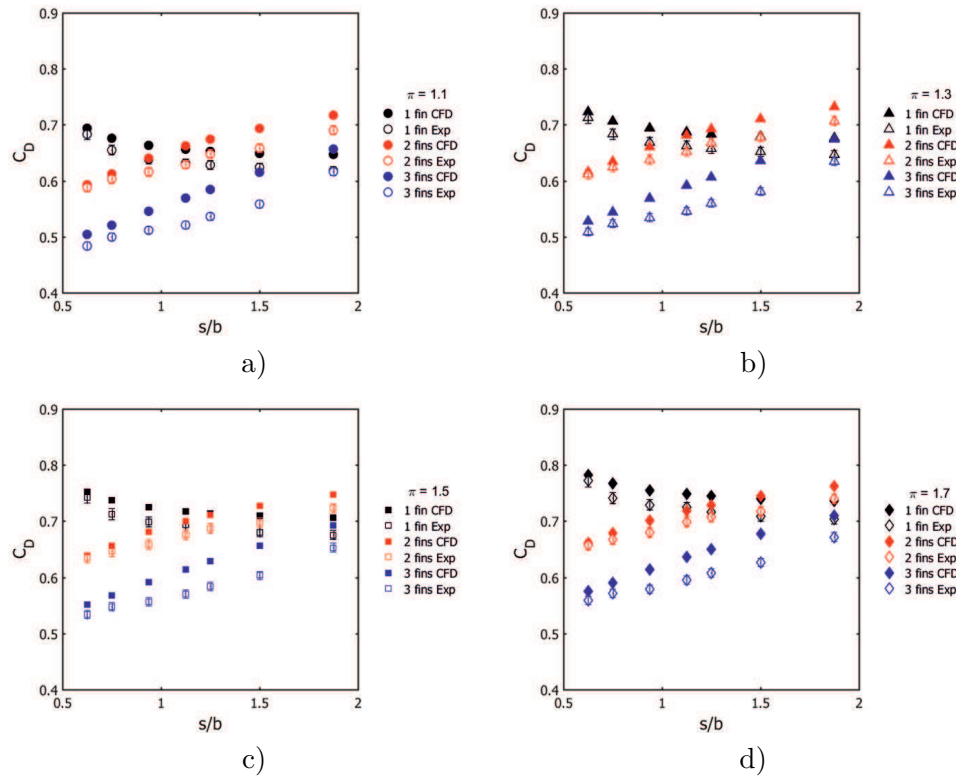


Figure 15: Discharge coefficient,  $C_D$ , as a function of relative clearance,  $s/b$ . Experiment and CFD results combined for all examined configurations a)  $\pi = 1.1$ , b)  $\pi = 1.3$ , c)  $\pi = 1.5$ , d)  $\pi = 1.7$ .

the later one, the air flows over the obstacle and detaches from the fin tip creating a counter-rotating vortex. The higher the gap is, the more space is left for the vortex to whirl, increasing the pressure loss. Because of that, the gap increase results in lower discharge coefficient. This phenomenon is the mechanism of flow reduction. On the other hand, in the case of a structure with two fins, there is a cavity created between them. Sometimes, in this situation, a carry-over effect occurs. It is a phenomenon taking place when some portion of kinetic energy is not dissipated in the seal and is ‘carried over’ to downstream components. It is strictly associated with the effectiveness of each cavity to dissipate the kinetic energy of fluid flowing into the cavity and affects the value of the discharge coefficient for the constriction following it. Clearance is one of the major geometric parameters that influence the carry-over coefficient for the structure, and therefore it is possible

that the configuration with one fin may be more effective in reducing the leakage than the configuration with more fins.

Described tendency illuminates a new fact – there are some areas where it could be more beneficial to apply simple design seal with only one fin instead of the more sophisticated seal with two fins. This would be reasonable in solutions with low-pressure load, and relatively high clearances – where the leakage is up to 15% lower for structure with one fin, than in more complex ones. The simpler design could also save time and manufacturing effort.

## 4 Summary

In this paper, a detailed study of aero engine intended straight-through labyrinth seals was presented. Authors focused on configuration with a low number of fins (one, two, and three). While the arrangement with one fin rarely occurs in the turbomachinery design, seals with two or three fins are often placed on stator or rotor blade shroud. On the other hand, many analytical codes are based on one fin configurations characteristics, for this reason, the information of the flow field in this structure is crucial.

The flow characteristics of non-dimensional flow indicators – discharge coefficient,  $C_D$ , and flow function  $\Psi$  were obtained using the in-house experimental vacuum test section, and commercial CFD code. The experiment performed on the test rig with non-moving circular specimens approach allowed for testing many different labyrinth seals configurations. Moreover, the circular shape of probes prove that the labyrinth seal circumference does not affect the mass flow rate. The CFD calculations adopt the quasi-2D RANS approach. Based on the detailed mesh and turbulence study, mesh with  $y^+ \approx 1$ , and  $k-\omega$  SST turbulence model was chosen for further inquiry. Proposed methodology showed satisfactory agreement concerning mass flow indicators. However, for the case with three fins, some discrepancies (up to 9%) were pointed out. Based on the research a significant validation of the literature data for one-finned labyrinth seal was presented – literature results presented the flow indicators 5–15% higher than those found in the study. This may have a source in some geometrical or physical variations. Cited results did not provide significant details about the thermodynamic parameters of the gas, with limited geometry data. On the other hand, all the trends and tendencies were reproduced as in the source data, which underlines the sensitivity of presented study. The study revealed an interesting tendency – one finned labyrinth seal presented different flow characteristics as seals with two and three fins – the discharge coefficient reduces as the clearance rises. To

the knowledge of authors, similar behaviour was not previously investigated in more details. The study additionally compared obtained results with flow characteristics of the seal with a higher number of fins (two and three), showing some operating conditions, where one finned seal provides the same, or even better flow reduction than structure with more fins.

Presented results may be of the interest for designers and researchers, dealing with secondary flows system in modern turbomachinery. In general, obtained flow characteristics for simple labyrinth seals can serve as data for validation and improvement of analytical methods, still commonly used for preliminary design purposes.

**Acknowledgements** The presented research was performed thanks to the Silesian University of Technology research funds.

## References

- [1] Steinetz B.M., Hendricks R.C., Braun M.J.: *Turbomachine Sealing and Secondary Flows. Part 1. Review of Sealing Performance, Customer, Engine Designer, and Research Issues*. NASA/TM – 2004-211991/Part1, Glenn Research Centre, Cleveland 2004.
- [2] Chupp R.E., Hendricks R.C., Lattime S.B., Steinetz B.M.: *Sealing in Turbomachinery*. NASA/TM – 2006-214341, Glenn Research Centre, Cleveland 2006.
- [3] Stocker H.L.: *Determining and Improving Labyrinth Seal Performance in Current and Advanced High Performance Gas Turbines*: Flow Systems Group, Detroit Diesel Allison, Indianapolis 1978.
- [4] Waschka W., Wittig S., Kim S.: *Influence of high rotational speeds on the heat transfer and discharge coefficients in labyrinth seals*. J. Turbomach. **114**(1992), 2, 462–468.
- [5] Paolillo R., Moore S., Cloud D., Glahn J.A.: *Impact of rotational speed on the discharge characteristic of stepped labyrinth seals*. In: Proc. GT2007 ASME Turbo Expo 2007: Power for Land, Sea and Air (2007), 1–8.
- [6] Braun E., Dullenkopf K., Bauer H.-J.: *Optimization of labyrinth seal performance combining experimental, numerical and data mining methods*. In: Proc. ASME Turbo Expo 2012: Turbine Technical Conf. Expo: Vol. 4, Heat Transfer, Pts. A and B, 1847–1854, 2012.
- [7] Rulik S., Wróblewski W., Fraczek D.: *Metamodel-based optimization of the labyrinth seal*. Arch. Mech. Eng. **64**(2017), 1, 75–91.
- [8] Wróblewski W., Dykas S., Bochon K., Rulik S.: *Optimization of tip seal with honeycomb land in lp counter rotating gas turbine engine*. Task Quart. **3**(2010), 3, 189–207.
- [9] Kang Y., Kim T.S., Kang S.Y., and Moon H.K.: *Aerodynamic performance of stepped labyrinth seals for gas turbine applications*. In: Proc. ASME Turbo Expo 2010: Power for Land, Sea and Air: Vol. 4: Heat Transfer, Pts. A and B, 1191–1199, 2010.
- [10] ] Massini D., Facchini B., Micio M., Bianchini C., Ceccherini A., and Innocenti L.: *Analysis of flat plate honeycomb seals aerodynamic losses: Effects of clearance*. Energy Procedia, **45**(2014), 502–511.

- [11] Zimmermann H., Wolff K.H.: *Air system correlations Part 1: Labyrinth seals*. In: Proc. Int. Gas Turbine and Aeroengine Cong. Exhib., 1–8, 1998.
- [12] Zimmermann H., Wolff K.H.: *Comparison between empirical and numerical labyrinth flow correlations*. In: Proc. ASME 1987 Int. Gas Turbine Conf. Exhib. Vol. 1, 1–6, 1987.
- [13] Kearton W.J., Keh T.H., Snow E.W.: *Leakage of air through labyrinth glands of staggered type – Discussion*. Proc. Inst. Mech. Eng. (1952), 180–195.
- [14] Weinberger T.: *Einfluss geometrischer Labyrinth- und Honigwabenparameter auf das Durchfluss- und Wärmeübergangsverhalten von Labyrinthdichtungen: Experiment, Numerik und Data Mining*. MSc dissertation, Karlsruher Institut für Technologie, Karlsruhe 2014.
- [15] Kim T.S., Kang Y., Moon H.K.: *Aerodynamic performance of double-sided labyrinth seals*. In: Proc. Int. Symp. on Fluid Machinery and Fluid Mechanics, 2008, 377–382.
- [16] Tipton D.L., Scott T.E., Vogel R.E.: *Labyrinth Seal Analysis: Vol. 3, Analytical and Experimental Development of a Design Model for Labyrinth Seals*. AFWAL-TR-85-2103: Vol. III, Allison Gas Turbine Division, Indianapolis 1986.
- [17] Szymanski A., Dykas S., Majkut M., Strozik M.: *The assessment of the calculation method for determining characteristics of one straight fin labyrinth seal*. Trans. Inst. Fluid-Flow Mach. **134**(2016), 89–107.
- [18] Szymanski A., Dykas S., Wróblewski W., Majkut M., Strozik M.: *Experimental and numerical study on the performance of the smooth-land labyrinth seal*. J. Phys.: Conf. Ser. **760**(2016), 1.
- [19] Frączek D., Wróblewski W., Chmielniak T.: *Influence of honeycomb rubbing on tip seal performance of turbine rotor*. ASME J. Eng. Gas Turb. Power **139**(2017), 1–13.
- [20] Choi D.-C., Rhode D.L.: *Development of a 2-D CFD approach for computing 3-D honeycomb labyrinth leakage*. ASME J. Eng. Gas Turb. Power **126**(2004), 794–802.
- [21] Kaszowski P., Dzida M.: *CFD analysis of fluid flow through the labyrinth seal*. Trans. Inst. Fluid-Flow Mach. **130**(2015), 71–82.
- [22] Kong X., Liu G., Liu Y., and Zheng L.: *Experimental testing for the influences of rotation and tip clearance on the labyrinth seal in a compressor stator well*. Aerosp. Sci. Technol. **71**(2017), 556–567.
- [23] Lin Z., Wang X., Yuan X., Shibukawa N., Noguchi T.: *Investigation and improvement of the staggered labyrinth seal*. Chin. J. Mech. Eng.-En. **28**(2015), 2, 402–408, .
- [24] Tyacke J.C., Jefferson-Loveday R., Tucker P.G.: *Application of LES to labyrinth seals*. In: Proc. 20th AIAA Computational Fluid Dynamics Conf., 2011, 1–24.
- [25] Tyacke J., Jefferson-Loveday R., Tucker P.G.: *On the application of LES to seal geometries*. Flow Turbul. Combust. **91**(2013), 4, 827–848.
- [26] CFX Tutorial, Chapter 9: Free Surface Flow Over a Bump.
- [27] Georgiadis N. Yoder D.: *Recalibration of the Shear Stress Transport Model to Improve Calculation of Shock Separated Flows*. NASA/TM-2013-217851, Glenn Research Centre, Cleveland 2013.
- [28] Menter F.R., Kuntz M., Langtry R.: *Ten years of industrial experience with the SST turbulence model*. Turbul. Heat Mass Transf. **4**(2003), 625–632.